EXTRACTING BUILDINGS FROM DIGITAL SURFACE MODELS

Ansgar Brunn, Uwe Weidner
Institut für Photogrammetrie
Rheinische Friedrich–Wilhelms-Universität Bonn
Nußallee 15, 53115 Bonn, Germany
Ph.: +49-228-732901, Fax: +49-228-732712
e-mail: ansgar;weidner@ipb.uni-bonn.de

KEY WORDS: Digital Surface Model, object detection, object reconstruction, Bayesian network

ABSTRACT

This paper describes an approach for building extraction using Digital Surface Models (DSM) as input data. The first task is the detection of areas within the DSM which describe buildings. The second task is the reconstruction of buildings for which we apply parametric and prismatic building models. The main focus is on the detection, namely on the use of height and differential geometric information to discriminate building and vegetation areas. Furthermore, recent results for the extraction of roof structures as first step towards the extraction of polyhedral building descriptions are presented.

1 INTRODUCTION

During the last years the increasing need for 3D data of urban areas und its update led to research efforts with the aim to set up automatic or at least semi-automatic tools for the acquisition of such data. Besides digital aerial images Digital Surface Models (DSM) are used as input data. DSM do not only contain information about the topographic surface like Digital Elevation Models (DEM), but also about buildings and other objects higher than the surrounding topographic surface, e.g. trees. The use of DSM for building extraction is motivated by the fact, that DSM already provide a geometric description of a scene derived from aerial imagery or airborne laser scanner data. Previously published approaches often use DSM for building detection only (e.g. Baltsavias et al., 1995). The inherent potential of DSM with respect to building reconstruction was explored only by a few authors, but either restricted to simple models (Haala, 1995) or by using additional input data (Jaynes et al., 1996). In our approach (c.f. Weidner and Förstner, 1995) we focus on the exclusive use of DSM in order to investigate the potential and – of course – limitations of DSM-analysis.

The applied criteria for building detection allow the separation of the two tasks of building detection and reconstruction. In the following, we therefore describe our approaches for both tasks focussing on new extensions: the discrimination of buildings and vegetation by use of differential geometry and the extraction of roof structures as first step towards the extraction of polyhedral building descriptions. In each section, we present the approach and also give examples of the results.

2 DISCRIMINATION OF BUILDINGS AND VEGETATION

Our approach for building detection exploits the fact, that the normalized DSM, i.e. the difference between DSM and Digital Elevation Model (DEM) describing the topographic surface, provides information about buildings approximately referenced to a plane. Therefore, the algorithm starts with the use of mathematical morphology to derive an approximation of the topographic surface, i.e. a DEM, from the DSM-data (Fig. 1[1]). The subsequent steps are to compute the normalized DSM, to binarize this data set using a global threshold yielding an initial segmentation $\tilde{\mathcal{S}}$, and to adapt the threshold based on local height information, which leads to the refined segmentation $\hat{\mathcal{S}}$ (Fig. 2). From these segments valid segments are selected based on their size in order to reject spurious segments, e.g. due to single trees (c.f. Weidner, 1997a for details). The size criterion for the selection is not sufficient for larger vegetation areas or vegetation areas close to buildings and probably melted together with these in the DSM. Assuming the geometric description provided by the DSM to be the only input data, criteria to classify vegetation areas must be geometric ones. A possible criterion is the roughness of the surface measured by differential geometric quantities, like gradients or curvatures. We exploit this information by computing step edges and the variance of surface normals as indicator for crease edges (Figure 3). This information is used via a binary classification scheme or Bayesian nets.

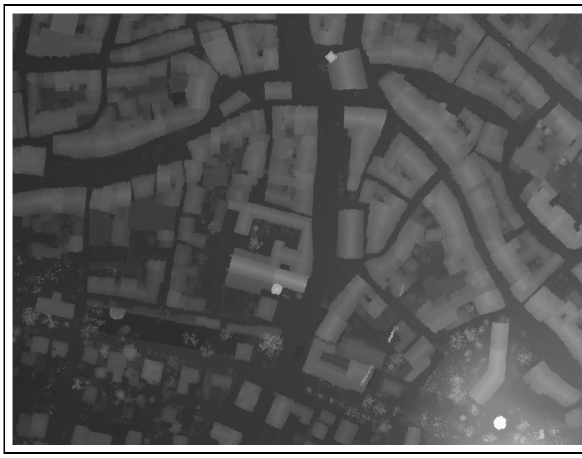

Figure 1: DSM RAVENSBURG

[1] The DSM RAVENSBURG was provided by TopoSys, Ravensburg.

Figure 2: Segments

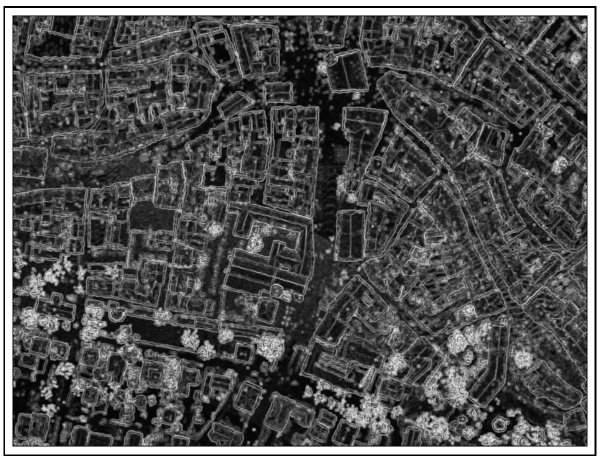

Figure 3: Variances of surface normals

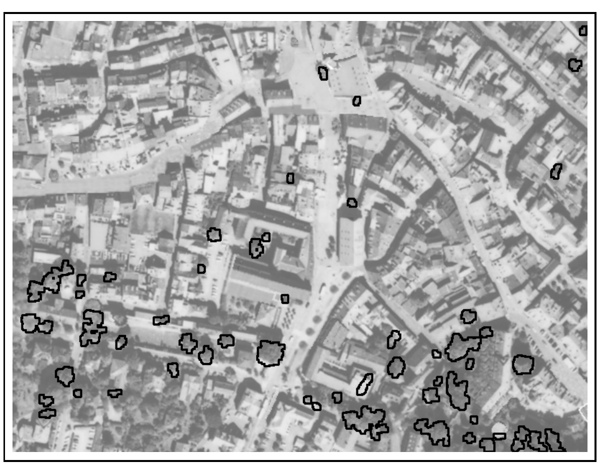

Figure 4: Detected vegetation areas $\hat{\mathcal{V}}$

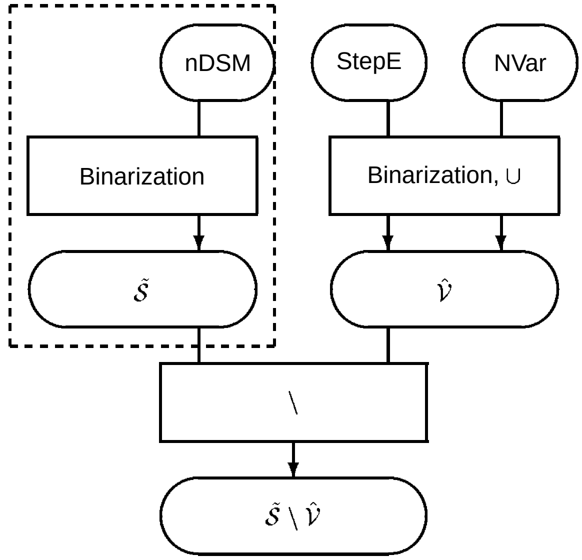

Figure 5: Binary Classification

2.1 Binary Classification Scheme

The detection of vegetation areas $\mathcal{V}$ within the DSM is an extension to the approach to building detection briefly outlined above. In the example vegetation areas can be easily recognized in the data sets of the step edges and crease edges (variance of surface normals, Figure 3). The first approach uses this informaton for a binary classification procedure (c.f. Figure 5). Besides the height information of the normalized DSM (dashed rectangle in Figure 5), the step and crease edge information is extracted (c.f. Weidner, 1997b for details) and classified using the expected roughness of vegetation as threshold. The entire procedure consists of binarizing the data sets, applying morphology in order to derive closed areas, and selecting valid vegetation segments $\hat{\mathcal{V}}$ by size evaluation. Figure 4 displays the detected vegetation areas. These areas can be excluded from the initial segmentation $\tilde{\mathcal{S}}$, thus replacing $\tilde{\mathcal{S}}$ by $\tilde{\mathcal{S}} \setminus \hat{\mathcal{V}}$.

The main drawback of the described approach is the use of fixed thresholds. This drawback can be overcome by using Bayesian networks for the classification instead of the binary classification scheme.

2.2 Bayesian Networks for Classification

In this section an approach for building detection and vegetation discrimination using Bayesian networks is proposed and evaluated. The approach is an extension of the work presented in Brunn et al., 1997, now using three different features: the height information from the normalized DSM Δh, the step edge magnitudes $StepE$ and the variances of surface normals $NVar$. For the description of the approach we will first focus on a subpart of the entire network circumscribed by the dashed rectangle in Figure 6, thus only considering the height information. It can replace the detection scheme briefly sketched at the beginning of this section. In a second step, the entire network is discussed.

Based on the features, pyramids of random variables $b_l = b_l(r, c, \mathbf{f})$ are generated, where r, c denotes the position, $\mathbf{f}$ the used group of features or the feature f, e.g. variance

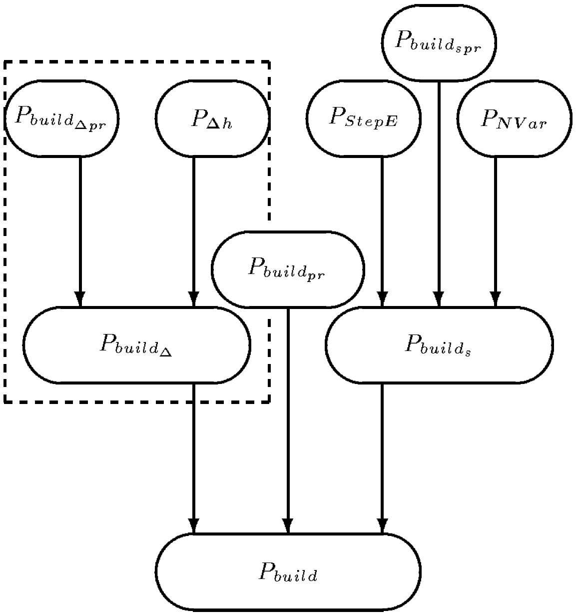

Figure 6: Bayes Classification

of surface normals, and l the level of the pyramid with $l = 0$ the original resolution of the data set. The probability that a point is member of a building region is denoted with $P(b_l(r,c) = \mathtt{T})$, the probability $P(b_l(r,c) = \mathtt{F})$, thus the probability of the complimentary event, is given by

$$P(b_l(r,c) = \mathtt{F}) = 1 - P(b_l(r,c) = \mathtt{T}) \tag{1}$$

The priori probabilities within the uni-directional Bayesian network are derived from the information of the next higher pyramid level, except for the highest level for which the priori probability must be given. The use of pyramids leads to regularization of the results. Furthermore, the influence of the selection of the priori probability for the highest level is reduced. For details of the computation of probabilities and the use of pyramids c.f. Brunn et al., 1997.

2.2.1 Using Height Information of Normalized DSM

In case the height of normalized DSM Δh is used as feature, the probability $P(b_l(r,c) = \mathtt{T})$, i.e. the point (r,c) is member of a building segment, follows from

$$\begin{aligned} &P(b_l(r,c) = \mathtt{T}) \propto \\ &\sum_{(\mathtt{S}_1,\mathtt{S}_2)} P(b_l(r,c) = \mathtt{T} | b_{l+1}(r,c) = \mathtt{S}_1, b_l(r,c,\Delta h) = \mathtt{S}_2) \\ &\qquad\qquad P(b_{l+1}(r,c) = \mathtt{S}_1) P(b_l(r,c,\Delta h) = \mathtt{S}_2) \end{aligned} \tag{2}$$

where the tupel $(\mathtt{S}_1, \mathtt{S}_2)$ has the values $\{(\mathtt{T},\mathtt{T}), (\mathtt{T},\mathtt{F}), (\mathtt{F},\mathtt{T}), (\mathtt{F},\mathtt{F})\}$. $P(b_{l+1}(r,c) = \mathtt{T})$ denotes the posterior probability derived on the $l+1$-th level of the pyramid, $P(b_l(r,c,f = \Delta h))$ the probability derived taking the feature on the l-th level into account, and $P(b_l(r,c)|b_{l+1}(r,c), b_l(r,c,\Delta h))$ the conditional probability. The probability $P(b_l(r,c,\mathbf{f}) = \mathtt{T}|\Theta)$ that a feature vector belongs to the region Θ in the feature space a priori defined by $\boldsymbol{\theta}$ and a covariance matrix $\mathbf{C}$ is calculated by

$$P(b(r,c)) = \frac{1}{\sqrt{2\pi \det \mathbf{C}}} \int_{\Theta} exp\left(-\frac{1}{2}(\mathbf{f}-\boldsymbol{\theta})^T \mathbf{C}^{-1}(\mathbf{f}-\boldsymbol{\theta})\right) \tag{3}$$

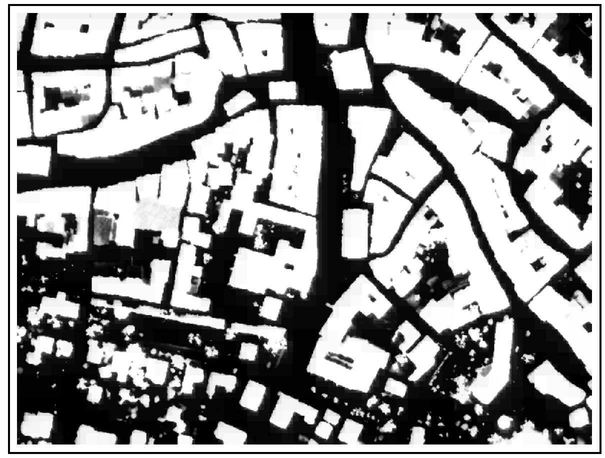

Figure 7: Probability of building segments

Figure 8: Classification of building segments

assuming normal distribution. For a single feature, e.g. Δh, and $\mathbf{C} = \sigma^2_{\Delta h}\mathbf{I}$, we obtain

$$P(b(r,c)) = \frac{1}{\sqrt{2\pi\sigma^2_{\Delta h}}} \int_{\Theta} exp\left(-\frac{(f-\theta)^2}{2\sigma^2_{\Delta h}}\right) \tag{4}$$

Thus, θ and $\sigma^2_{\Delta h}$ have to be defined instead of a threshold for the approach described above. The first parameter can be set analogously to the threshold based on object knowledge, the second taking the sensor model into account. The conditional probabilities $P(A|B)$ have to be fixed by the user and express the belief in A under the assumption that B is given. For the results displayed in Figures 7 and 8 we used

$$\begin{aligned} P(b_l(r,c) = \mathtt{T}|b_{l+1}(r,c) = \mathtt{T}, b_l(r,c,\Delta h) = \mathtt{T}) &= 1.00 \\ P(b_l(r,c) = \mathtt{T}|b_{l+1}(r,c) = \mathtt{F}, b_l(r,c,\Delta h) = \mathtt{T}) &= 0.50 \\ P(b_l(r,c) = \mathtt{T}|b_{l+1}(r,c) = \mathtt{T}, b_l(r,c,\Delta h) = \mathtt{F}) &= 0.50 \end{aligned} \tag{5}$$

and zero for the last of the conditional probabilities in (2) expressing belief only if both random variables are true $\mathtt{T}$. Based on the probability of buildings (Figure 7, white: high probability) the classification with $P_{build} > 0.5$ for the last pyramid level, i.e. the original resolution, yields the building segments (Figure 8, black) leading to almost the same results as the detection scheme described at the beginning of this section, but already rejecting smaller areas due to the use of pyramids and the inherent smoothing and delivering also information about the probabilities.

Figure 9: Probability of building segments using normalized DSM and differential geometric properties

Figure 10: Classification $\tilde{\mathcal{S}}_B$ of building segments using normalized DSM and differential geometric properties

2.2.2 Using Height Information and Differential Geometric Properties

Taking the binary classification scheme described in Section 2.1 as starting point, a Bayesian network for the discrimination of building and vegetation areas can be formulated as presented in Figure 6. The equations for the probabilities follow analogously to (2). The probabilities P_{StepE} and P_{NVar} of the l-th level for each point are computed as median probability within a 3×3 neighbourhood which can be compared to the use of mathematical morphology in the binary classification scheme. The strict thresholds within the binary classification are replaced by the parameter vector $\boldsymbol{\theta}$ and its covariance matrix $\mathbf{C}$. In our experiments we assumed uncorrelated sources, thus $\mathbf{C}$ is a diagonal matrix with entries $\sigma^2_{f_i}$. The conditional probabilities express the belief and can be used to put more emphasis on a specific source of information. The main advantage of the Bayesian network is the fact, that information about the probability of classification for each point is provided.

For the computation of the probability P_{build_Δ} (c.f. Figure 6) the conditional probabilities given in (5) are used. The conditional probabilities used for the computation of P_{build_s} are selected analogously but also taking the number of variables $b = T$ and the belief in differential geometric properties of a higher level into account. The same holds for the conditional probabilities for the computation of P_{build}. Details are given in Brunn and Weidner, 1997.

Figures 9 and 10 display the probabilities P_{build} and the related classifications for several pyramid levels. For comparision the result $\tilde{\mathcal{S}} \setminus \hat{\mathcal{V}}$ of the binary classification scheme is given in Figure 11 and the difference of the classifications is presented in Figure 12. Within this data set white segments represent building segments which are not detected using the binary classification scheme but using the approach based on the Bayesian network. Black regions represent just the opposite cases and grey regions mark regions with no differences. The Bayesian approach leads to the detec-

Figure 11: Segments $\tilde{\mathcal{S}} \setminus \hat{\mathcal{V}}$

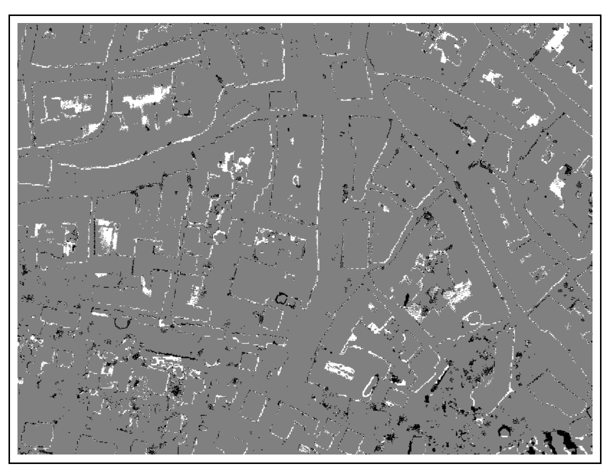

Figure 12: Differences of $\tilde{\mathcal{S}} \setminus \hat{\mathcal{V}}$ and $\tilde{\mathcal{S}}_B$

tion of buildings with low heights in backyards (e.g. white segments in NW part of data set), which are not detected by binary classification due to the strict thresholding. In case the Bayesian network scheme is used, the threshold used in the binary scheme – which is set also to avoid detection of vegetation (bushes) – can be relaxed. Furthermore segments in the SE part are correctly rejected. Differences along segment borders are of minor significance.

For the example the Bayesian approach is superior to the binary classification due to the mentioned characteristics. Both approaches require high quality data, i.e. minor effects due to regularization. A counter example for the approaches is given by the DSM AVENCHES (Figure 13): a group of trees (NE part of data set) appears as smooth as building segments (Figure 14). Therefore, the probabilities P_{build_s} are almost constant and > 0.9 indicating that in this case the differential geometric properties do not carry any significant information for the discrimination between building and vegetation areas and leading to the result shown in Figure 15. This result does not significantly differ from the result obtained using the height information of the normalized DSM only (Figure 16).

3 EXTRACTION OF ROOF STRUCTURES

In our previously published work on building extraction using DSM as input data we only applied parametric and prismatic building models. These models are not sufficient with respect to complex scenes like downtown areas with complex buildings. Therefore, we will integrate polyhedral models in our approach. This integration does not change the general framework, because the models applied up to now are subclasses of polyhedral models derived by imposing restrictions on the topology and/or metric. The first step towards the extraction of polyhedral models is the extraction of roof planes.

The principle idea is to extract homogeneous, i.e. planar, regions within the detected building segments. Like most approaches to range image segmentation (c.f. Arman and Aggarwal, 1993), we also focus on the extraction of regions. The data $\mathcal{D}$ consist of points which either belong to mutually exclusive homogeneous regions $\mathcal{R} = \{\mathcal{R}_1, \ldots \mathcal{R}_r\}$ and $\forall i \neq j \; \mathcal{R}_i \cap \mathcal{R}_j = \emptyset$ or to the set $\mathcal{E}$ of non-homogeneous regions, i.e. edges or discontinuities. Thus,

$$\mathcal{D} = \mathcal{R} \cup \mathcal{E} \tag{6}$$

The discontinuities – borders of planar patches – are indicated either by depth changes in surface normal direction or high curvature, which is related to changes of the surface normals. Therefore, we start with the computation of the surface normals $n_{i\cdot}$ with $i \in \{1, 2, 3\}$ denoting its components in x, y and z. Filtering of these surface normals is necessary in order to reduce the influence of noise on the results of following steps. The use of linear filters – as e.g. included in Hoffman and Jain, 1987 – leads to deterioration of information about discontinuities. Therefore, adaptive techniques should be applied. We have chosen a filter based on adaptive masks using a maximum homogeneity criterion. It is a modification of the filter presented by Nagao and Matsuyama, 1979 using the variance of surface normals as homogeneity criterion, thus quite similar to the USF-segmenter included in Hoover et al., 1996 with respect to the used neighbourhoods. Figures 17 and 18 display the discontinuity maps computed based on the unfiltered

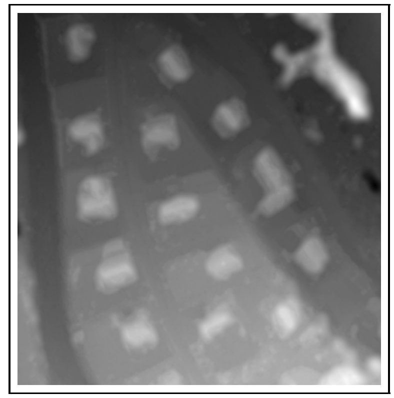

Figure 13: DSM AVENCHES

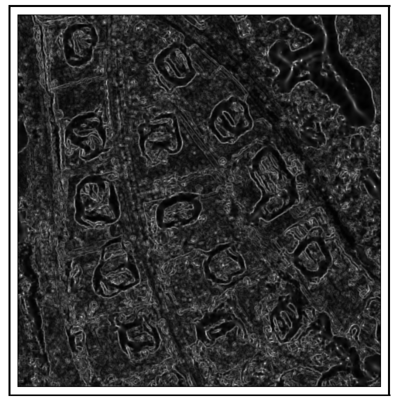

Figure 14: Variances of surface normals

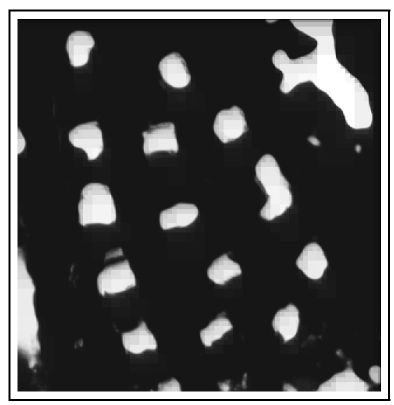

Figure 15: Probability of building segments using normalized DSM and differential geometric properties

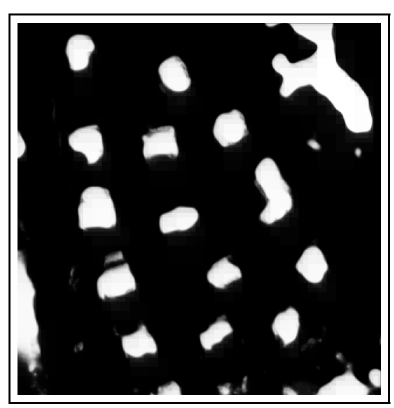

Figure 16: Probability of building segments using normalized DSM

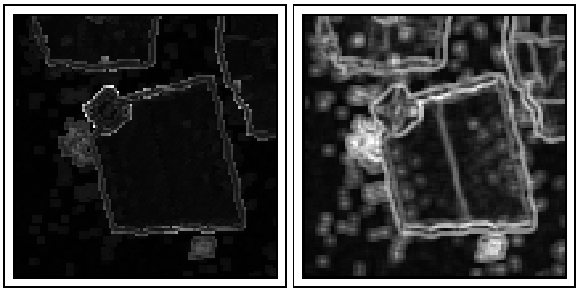

Figure 17: Discontinuities

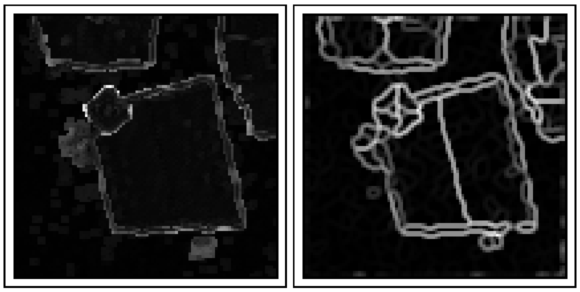

Figure 18: Discontinuities after filtering

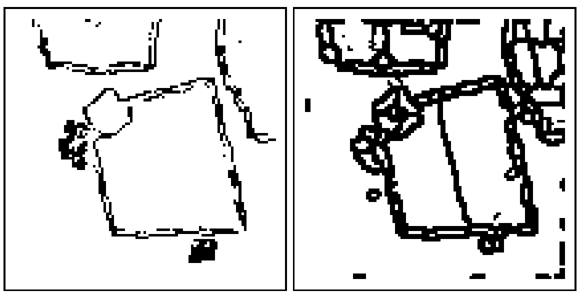

Figure 19: Detected discontinuities

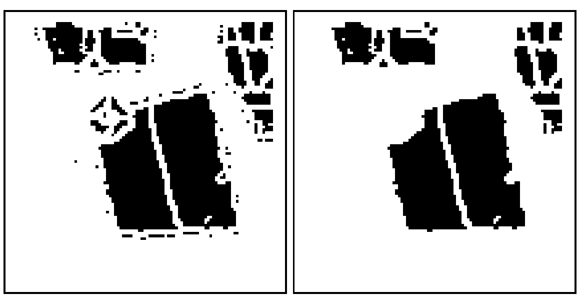

Figure 20: Detected and selected roof segments

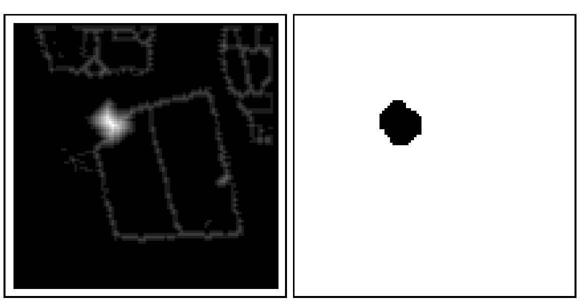

Figure 21: Non-recovered areas

	21	22	24	28	29	30	32	34	39	40
21	●		⊙ ⊕	∘						
22		●	∘							
24	⊙ ⊕	∘	●	∘		∘		⊙ ⊕	∘	
28	∘		∘	●	∘					
29				∘	●		∘	⊖		
30			∘			●				
32					∘		●	∘		
34			⊙ ⊕		⊖		∘	●	∘	∘
39			∘					∘	●	
40								∘		●

● (diagonal) ⊙ slope ⊕ symmetric
∘ neighbour ⊖ antisymmetric

Table 1: Hypotheses about regularities

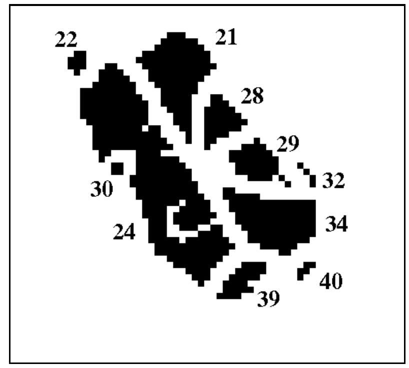

Figure 22: Selected roof labels

and filtered surface normals. Binarization of the discontinuity maps yields the significant discontinuities (Fig. 19). For this binarization thresholds have to be fixed. These threshold can be derived using knowledge about objects and considering the requirements of a special task. Examples for user specifications are height differences between roof parts and for knowledge the expected minimal slope of roofs, which can be used to compute an expected variance of normals at ridges. The detected discontinuities define set $\hat{\mathcal{E}}$ in (6). The planar segments are the complimentary set, thus $\tilde{\mathcal{R}} = \mathcal{D} \setminus \hat{\mathcal{E}}$. If the buildings are already detected, the set $\mathcal{D}$ may be replaced by the set of selected building segments $\hat{\mathcal{S}}$, thus $\tilde{\mathcal{R}}$ are the detected roof segments. The result of segmentation is a classification of points. These points can be grouped by determining connected components and labelled. From the detected initial roof segments $\tilde{\mathcal{R}}$ (Fig. 20, left) valid segments $\hat{\mathcal{R}}$ are selected based on their size – at least 3 non-collinear points – and their slope (Fig. 20, right). The slope criterion is used to reject areas due to round offs within the DSM. Due to the rejection of detected segments, areas within the building segments which are not covered by valid planar roof segments $\hat{\mathcal{R}}$ may occur. These areas $\mathcal{R}^*$ are detected by analysis of the distance image (Fig. 21) and may consist of higher order surfaces.

Up to now the parameters for each detected valid roof segment $\hat{\mathcal{R}}_i$ are estimated separately. Note that the afore mentioned filtering is used as preprocessing in order to obtain hypotheses about roof segments. The evaluation of these segments is performed using the original data. Based on the neighbourhood relations and the estimated parameters hypotheses about regularities are derived locally (c.f. Tab. 1 for the example displayed in Fig. 22). Examples for such regularities between two planes A and B are the slope

$$d^{(sl)} = n_{3.B} - n_{3.A} = 0 \tag{7}$$

and the orientation, thus parallel

$$d^{(p*)}_{\alpha.} = n^*_{\alpha.B} - n^*_{\alpha.A} = 0_{\alpha.} \tag{8}$$

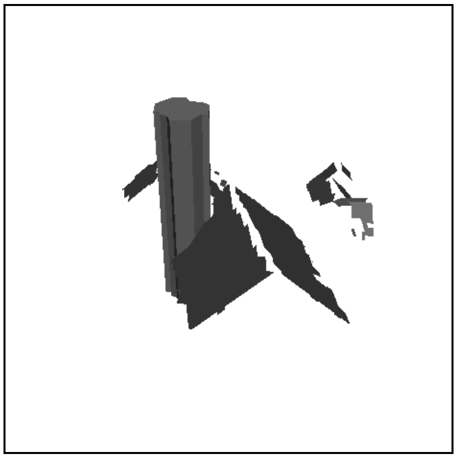

Figure 23: Reconstructed roof structure

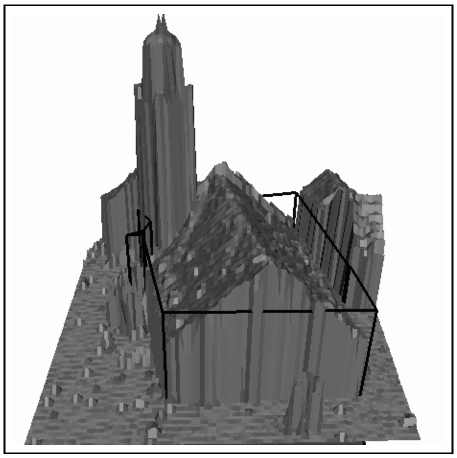

Figure 24: Data and prismatic model

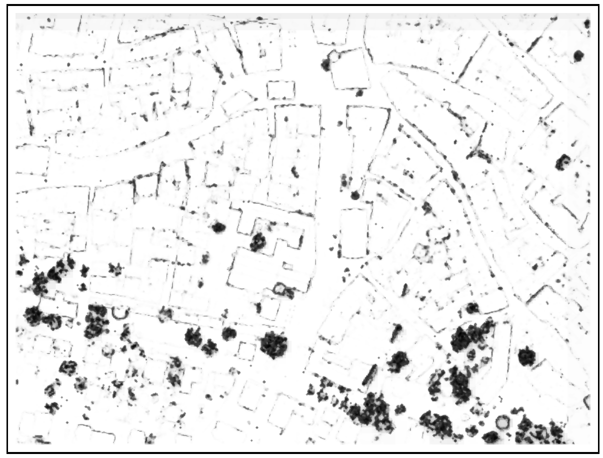

Figure 25: Probabilities P_{build_s}, $\theta_{NVar} = 1.0$

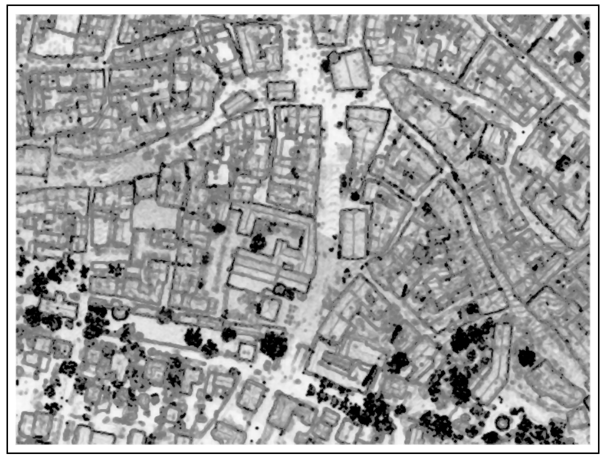

Figure 26: Probabilities P_{build_s}, $\theta_{NVar} = 0.1$

symmetric

$$d_{\alpha.}^{(s*)} = n_{\alpha.B}^{(s)} - n_{\alpha.A}^{*} \tag{9}$$

and antisymmetric

$$d_{\alpha.}^{(a*)} = n_{\alpha.B}^{(a)} - n_{\alpha.A}^{*} \tag{10}$$

with $\alpha, \beta \in \{1, 2\}$,

$$n_{\alpha.}^{*} = \frac{n_{\alpha.}}{\| n_{\beta.} \|} \quad , \quad n_{\alpha.}^{(s)} = -n_{\alpha.}^{*} \quad \text{and} \quad n_{\alpha.}^{(a)} = \begin{pmatrix} -n_{2.}^{*} \\ n_{1.}^{*} \end{pmatrix}$$

These hypotheses will be integrated in a global robust adjustment and evaluated analogously to the approach for polygon reconstruction of the building outlines (Brunn et al., 1995). The segments $\mathcal{R}^*$ are up to now described by planes with constant heights (Fig. 23). Further refined reconstruction is necessary, e.g. using higher order surfaces (Leonardis, 1993).

4 CONLUSIONS AND FURTHER WORK

In this contribution we focussed on new extensions of our approach for building extraction from DSM, namely the discrimination of building and vegetation areas using differential geometric properties of the surfaces and roof extraction as first step towards the extraction of polyhedral building descriptions.

We presented two schemes for building detection including detection of vegetation in DSM. The first scheme is based on a binary classification scheme, the second on Bayesian networks. Both approaches take the height information and differential geometric properties of the surface into account. Therefore, both require high quality data with respect to the differential geometric properties. These requirements are not always fulfilled. Nevertheless, the investigations indicate that different sources of information can be analysed by use of Bayesian networks as common framework. In order to discriminate between building and vegetation areas, the Bayesian network can be extended by integrating other sources of information, e.g. reflectance properties derived by analysis of the intensity of returned laser signals (c.f. Hug, 1997) and information from digital images, e.g. texture and/or colour (c.f. Eckstein and Munkelt, 1995). Further work in this field may also extend to roof plane extraction using the Bayesian net for their detection. Figures 25 and 26 show the probabilities P_{build_s} related to two different parameters θ_{NVar}. In the first case θ_{NVar} was set in order to reject vegetation areas, in the second case with respect to detect planar surfaces. For this purpose the filtered surface normals may be used for the computation of step edges and the variance of surface normals. Further investigations are necessary.

The presented approach for roof extraction from DSM aims at the extraction of polyhedral building descriptions. The task consists of two subtasks: roof plane detection and roof plane reconstruction. The roof plane detection is focused on detected building segments and uses differential geometric properties to detect depth and normal discontinu-

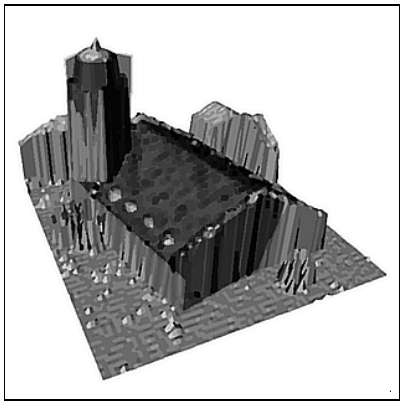

Figure 27: Semi-automatically measured building model

ities. The derived discontinuity maps are combined with the building segments. This combination yields the initial roof segments $\tilde{\mathcal{R}}$. Geometrical criteria, i.e. number of points and slope, are used to select valid roof segments $\hat{\mathcal{R}}$, which are used for the reconstruction.

The first step for the reconstruction is the estimation of parameters for each plane. Based on these parameters hypotheses about regularities are automatically detected. These regularities deliver constraints for further reconstruction applying a global estimation with constraints.

Up to now, the roof segmentation and the roof reconstruction including the first parameter estimation and the derivation of hypotheses are implemented. The obtained results are promising. Further work will focus on robust estimation of plane parameters without and with constraints. Furthermore, consistency checks of the hypotheses with respect to the object model should be investigated in order to detect contradictory and inconsistent hypotheses. This also includes the use of groundplan information, either extracted from the DSM or provided by GIS (c.f. Haala and Brenner, 1997).

Using polyhedral models and thereby planes for roof extraction is limited, which is indicated by the examples. Therefore, regions of the building segments, which are not covered by the extracted roof planes, must be treated separately, e.g. using higher order surfaces (c.f. Leonardis, 1993).

Automatic procedures may fail in recovering the correct information due to the complexity of the task. Therefore, interactive tools for editing the results are necessary. For this purpose our approach to semi-automatic building extraction from digital images will be extended for DSM (Gülch, 1997). A first result – an overlay of extracted model and original data – is shown in Figure 27.

REFERENCES

Arman, F. and Aggarwal, J. K., 1993. Model-Based Object Recognition in Dense-Range Images – A Review. ACM Computing Surveys 25(1), pp. 5–43.

Baltsavias, E., Mason, S. and Stallmann, D., 1995. Use of DTMs/DSMs and Orthoimages to Support Building Extraction. In: A. Grün, O. Kübler and P. Agouris (eds), Automatic Extraction of Man-Made Objects from Aerial and Space Images, Birkhäuser, Basel, pp. 199–210.

Brunn, A. and Weidner, U., 1997. Discriminating Building and Vegetation Areas within Digital Surface Models. Technical Report IPB-97/2, Institut für Photogrammetrie, Bonn.

Brunn, A., Gülch, E., Lang, F. and Förstner, W., 1997. A Multi-Layer Strategy for 3D Building Acquisition. In: Mapping Buildings, Roads and other Man-Made Structures from Images, Proceedings IAPR TC-7 Workshop Sept. 2-3, 1996, Graz, Oldenbourg, Wien/München, pp. 11–37.

Brunn, A., Weidner, U. and Förstner, W., 1995. Model-based 2D-Shape Recovery. In: G. Sagerer, S. Posch and F. Kummert (eds), Mustererkennung 1995, DAGM, Springer, pp. 260–268.

Eckstein, W. and Munkelt, O., 1995. Extracting Objects from Digital Terrain Models. In: T. Schenk (ed.), Remote Sensing and Reconstruction for Three-Dimensional Objects and Scenes, SPIE.

Gülch, E., 1997. Application of Semi-Automatic Building Acquisition. In: A. Grün (ed.), Automatic Extraction of Man-Made Objects from Aerial and Space Images (II), Birkhäuser, Basel.

Haala, N., 1995. 3D Building Reconstruction Using Linear Edge Segments. In: D. Fritsch and D. Hobbie (eds), Photogrammetric Week, Wichmann, Karlsruhe, pp. 19–28.

Haala, N. and Brenner, C., 1997. Integration of GIS and Images for Building Reconstruction. In: A. Grün (ed.), Automatic Extraction of Man-Made Objects from Aerial and Space Images (II), Birkhäuser, Basel.

Hoffman, R. and Jain, R. C., 1987. Segmentation and Classification of Range Images. IEEE T-PAMI 9(5), pp. 608–620.

Hoover, A., Jean-Baptiste, G., Jiang, X., P.J.Flynn, nad D. Goldgof, H. B., Bowyer, K., Eggert, D., Fitzgibbon, A. and Fisher, R., 1996. An Experimental Comparison of Range Image Segmentation Algorithms. IEEE T-PAMI 18(7), pp. 673–689.

Hug, C., 1997. Extracting Artificial Objects from Airborne Laser Scanner Data. In: A. Grün (ed.), Automatic Extraction of Man-Made Objects from Aerial and Space Images (II), Birkhäuser, Basel.

Jaynes, C., Stolle, F., Schultz, H., Collins, R. T., Hanson, A. and Riseman, E., 1996. Three-Dimensional Grouping and Information Fusion for Site Modelling from Aerial Images. In: ARPA Image Understanding Workshop, Palm Springs,CA, Proceedings.

Leonardis, A., 1993. Image Analysis Using Parametric Models. PhD thesis, Faculties of Electrical Engineering and Computer Science, University of Ljubljana.

Nagao, M. and Matsuyama, T., 1979. Edge Preserving Smoothing. CGIP 9, pp. 394 ff.

Weidner, U., 1997a. Gebäudeerfassung aus Digitalen Oberflächenmodellen. C, Vol. 474, Deutsche Geodätische Kommission, München.

Weidner, U., 1997b. Roof Extraction from Digital Surface Models. Technical Report IPB-97/1, Institut für Photogrammetrie, Bonn.

Weidner, U. and Förstner, W., 1995. Towards Automatic Building Extraction from High Resolution Digital Elevation Models. ISPRS Journal 50(4), pp. 38–49.